A Single Stage Flyback Power Supply Unit for LED lighting Applications

Jae-Eul Yeon[1], Dong-Soo Kim[1], Kyu-min Cho[2] and Hee-Jun Kim[3]

[1] Visual System Team, HV_PCIA, Fairchild Korea Semiconductor, Korea,
jaeeul.yeon@fairchildsemi.com, dongsoo.kim@fairchildsemi.com
[2] Department of Information and Communications, Yuhan University, Korea, limsa@yuhan.ac.kr
[3] School of Electrical and Computer Engineering, Hanyang University, Korea, hjkim@hanyang.ac.kr

Abstract

This paper presents a 75W single-stage power supply unit for LED lighting. The proposed power supply designed using flyback converter topology that is controlled by the critical conduction mode control. The secondary side of main transformer is directly connected to LED strings. By a constant current feedback circuit, this flyback converter directly regulates LED current. Although the proposed circuit doesn't need input current-sensing and input voltage feed-forward, it can achieve high power factor for wide input range. A prototype experimental set-up has been built and tested. Through this experiment with a prototype set-up, the validity of the proposed circuit is verified.

1. Introduction

In recent years, LED technology has been grown rapidly and it is considered as a most strong candidate for the next generation lighting source due to high energy efficiency, long life time and its positive environmental attributes. Moreover, LED technology controls the color, shape, illumination pattern as well as light itself [1]. In the case of indoor or street LED lighting application, a power supply unit(PSU) that converts AC input voltage to DC output voltage is necessary and various topologies have being considered [2-4]. The PSUs for low power LED lighting are normally single-stage converter types but two stage converters are common for a high power LED lighting applications due to their power limitation. In this paper a single-stage PSU for high power LED lighting is presented. As the power converter circuit, flyback converter topology is applied because it doesn't need an inductive output filter, the main transformer works as an inductive filter itself and the input and output stages can be isolated [5, 6]. The proposed circuit used a critical conduction mode (CRM) PFC controller and the input voltage and switching current are not needed, the only output voltage feed-back is necessary. Through an experiment with a prototype 75W single stage flyback converter, the feasibility of the proposed single stage PSU, control scheme and feedback methods are examined and discussed in this paper.

2. Single Stage Flyback Converter for LED

2.1 Fundamental analysis

Figure 1 shows the circuit diagram of a flyback AC-DC converter. Both CV(constant voltage) and CC(constant current) feedback circuit are needed to prevent overload condition as well as over voltage conditions. In LED lighting, the output is always full load condition and the forward voltage drop of LED will be decreased in accordance with the increasing junction temperature of LED. Therefore the output should be controlled
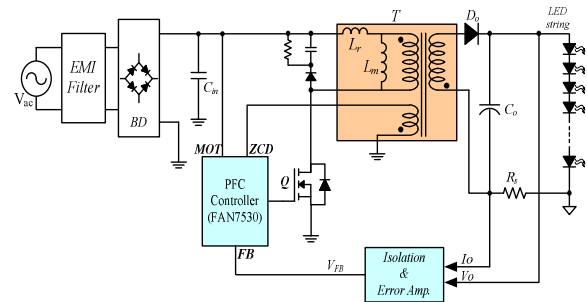

Fig. 1. Circuit diagram of a flyback AC-DC converter

by CC mode in the normal state while CV mode only acts as over voltage protection.

A voltage mode CRM PFC controller, FAN7530 is used as a control IC and the internal block diagram is shown in Figure 2. In the control circuit, the switching signal is generated by comparing the output of the error amplifier with the internal ramp signal. Consequently, the input voltage and current are unnecessary. The turn-on time of switch is fixed while the turn-off time is varied during the steady state. Therefore, the switching frequency inevitably varies in accordance with the input voltage variation as shown in Figure 3.

Figure 4 illustrates the theoretical waveforms of the primary side switch current, the secondary side diode current and gating signal. MOSFET, Q turns on and FRD, D_o turns off under zero-current condition while Q turns off and D_o turns on under the hard switching condition.

In flyback converter, the transformer will be easily saturated because the transformer is only utilized within 1st quadrant. Moreover if it works under the critical conduction mode, the peak current is much higher than that of the continuous conduction mode. Therefore the air-gap should be inserted to
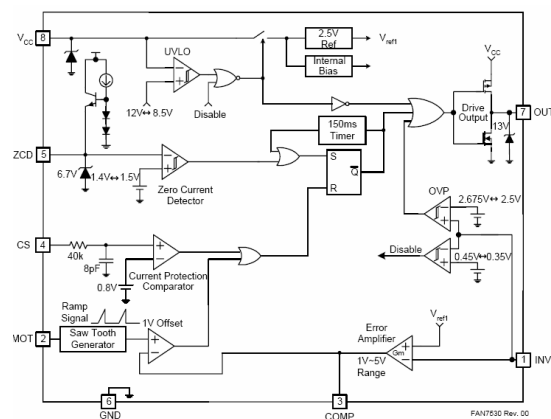
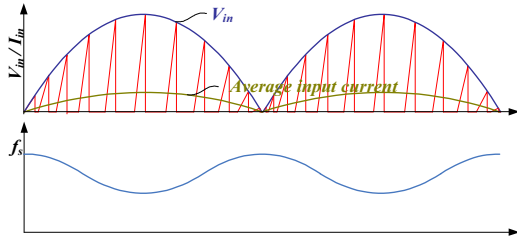

Fig. 2. Block diagram of FAN7530
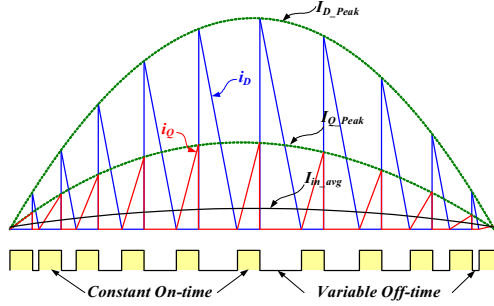
Fig. 3. Switching frequency variation

Fig. 4. Theoretical waveforms

prevent the saturation of the transformer.

When a flyback converter is applied to the single stage AC-DC converter, the proper turn ratio, N_2/N_1, is very important because the maximum voltage rating of MOSFET and FRD strongly relates with the turn ratio of transformer. There is a trade off relationship between the drain to source voltage rating, V_{dss}, of MOSFET and the reverse voltage rating, V_R of FRD according to the turn ratio of the transformer. The larger turn ratio requires the higher DC reverse voltage, V_R of FRD while the drain-source voltage, V_{dss}, of MOSFET is decreased. In contrast, the lower turn ratio causes the higher voltage stress of MOSFET while V_R of FRD is decreased.

Figure 5 shows the trade-off relationship between V_{dss}, of MOSFET and V_R of FRD. From $P_o=\eta V_{in}I_{in}$, the maximum input current, $I_{in(max)} = P_o/\eta V_{in}$. If the switching frequency, f_s is much higher than the AC line frequency, f_{ac}, the input current can be assumed to be constant during a switching period.

In order to define the magnetizing inductance of transformer, the longest period has to be defined. The longest switching period occurs at the peak point of the input current when the minimum input voltage is applied. The maximum input current and the switching peak current is defined as follow;

Table 1. Electrical parameters

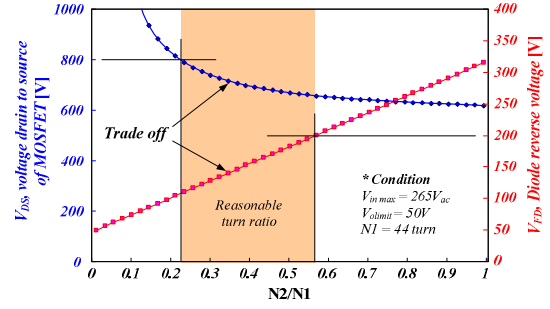| Parameters	Value
Output Power	75W
Input Voltage Range	85-265V
Output Voltage	45V
Limited output voltage	50V
Turn ratio (N2/N1)	17/44
Magnetizing inductance	297uH
Minimum switching frequency, $f_{s\_min@\,Vin\_min}$	50kHz
Efficiency, η	85 %

Fig. 5. V_{DS} and V_R in accordance with turn ratio

$$I_{in(max)\_pk} = \frac{\sqrt{2}P_o}{\eta V_{i\_min}} = \frac{1}{T}\int_0^{DT}\frac{I_{Q\_pk}}{D_{max}T}t\,dt = \frac{D_{max}}{2}I_{Q\_pk} \quad (1)$$

$$I_{Q(max)\_pk} = \frac{2}{D}I_{in(max)\_pk} = \frac{2\sqrt{2}P_o}{\eta D_{@\,Iin(max)\_pk}V_{in(min)}} \quad (2)$$

Where, $I_{in(max)\_pk} = \sqrt{2}I_{in(max)}$ and $V_{in(min)\_pk} = \sqrt{2}V_{in(min)}$ respectively.

The transformer primary side voltage, V_T is defined as follow;

$$V_T = L_m\frac{\Delta I}{\Delta T} = L_m\frac{I_{Q(max)\_pk}f_{s(min)}}{D_{@\,Iin(max)\_pk}} \quad (3)$$

Therefore, the magnetizing inductance is obtained as follow;

$$L_m \geq \frac{D_{@\,Iin(max)\_pk}^2 V_{in(min)}}{2I_{in(max)\_pk}f_{s(min)}} \quad (4)$$

The voltage stress of MOSFET is

$$V_{ds(max)} = V_{in(max)\_pk} + V_{sn(max)}$$
$$= V_{in(max)\_pk} + V_f + V_{Lr} \quad (5)$$

where V_{sn} is the maximum capacitor voltage of the snubber circuit, $V_f(N_1V_o/N_2)$ is the flyback voltage and V_{Lr} is the ringing voltage at the leakage inductance of the transformer respectively. Normally V_{Lr} is estimated as 1.5 times of the flyback voltage. The maximum reverse voltage and the forward peak current of FRD are

$$V_{R\,max} = V_{o\_Limit} + \frac{N_2}{N_1}V_{i\_pk(max)} \quad (6)$$

$$I_{R\_pk} = \frac{2}{\left(1 - D_{@\,Iin(max)\_pk}\right)}I_o \quad (7)$$

respectively.

2.2 Snubber circuit design

In flyback converter, the resonant between L_{leak} and C_{oss} occurs an excessively high voltage surge which causes the damage of MOSFET during the turn-off instant. This voltage surge has to be suppressed and the snubber circuit is therefore necessary to prevent MOSFET failures as shown in Figure 6.

The clamping voltage by snubber is

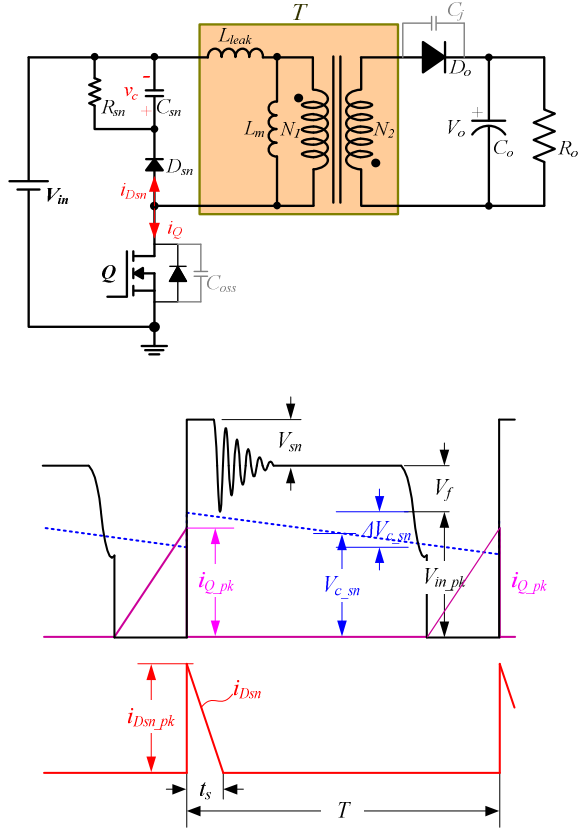$$V_{sn} = V_f + L_{leak}\frac{\Delta i}{\Delta t} = V_f + L_{leak}\frac{I_{Dsn\_pk}}{t_s} \quad (8)$$

Fig. 6. Snubber circuit design

Therefore,

$$t_s = \frac{L_{leak} \times I_{Dsn\_pk}}{V_{sn} - V_f} = \frac{L_{leak} \times I_{Dsn\_pk}}{1.5V_f} \quad (9)$$

The maximum power dissipation of the snubber circuit is determined by

$$P_{sn} = \frac{1}{T}\int_0^{t_s} V_{sn} i_{Dsn}(t) dt = \frac{1}{2} L_{leak} I_{Dsn\_pk}{}^2 f_s \quad (10)$$

and, the maximum power dissipation is

$$P_{sn(\max)} = \frac{1}{2} L_{leak} I_{Dsn\_pk}{}^2 f_{s@vin\max} = \frac{v_c{}^2}{R_{sn}} \quad (11)$$

Where, $v_c = V_f + V_{sn}$. Therefore, the resistance, R_{sn} is determined by

$$R_{sn} = \frac{2v_c{}^2}{L_{leak} I_{Dsn\_pk}{}^2 f_{s@vin\max}} \quad (12)$$

The maximum ripple voltage of snubber circuit is obtained as follow;

$$\Delta v_c = \frac{v_c}{C_{sn} R_{sn} f_{s@vin\max}} \quad (13)$$

The larger snubber capacitor results the lower voltage ripple, but the power dissipation will be increased. Consequently, selecting the proper value is important. In general, it is reasonable to determine that the snubber voltage is 1.5 times of the flyback voltage and the ripple voltage is 50V.

3. Experimental Results

To verify the validity of the proposed circuit, a prototype 75W experimental set-up has been built and tested.
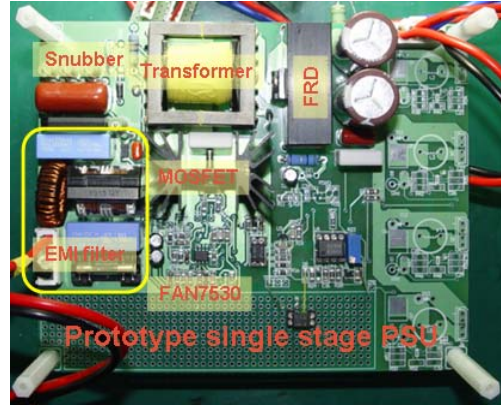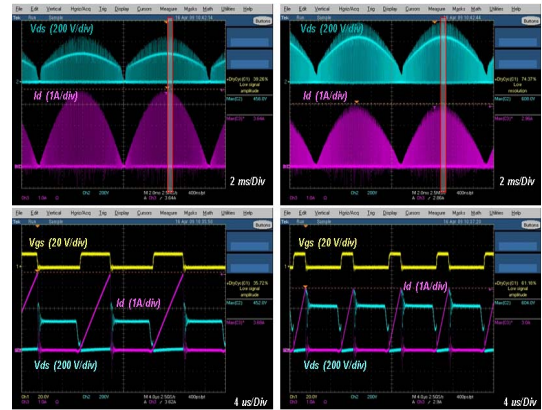

Fig. 7. Photograph of 75W prototype experimental set-up

(a) at 110 V_{ac} input (b) at 220 V_{ac} input

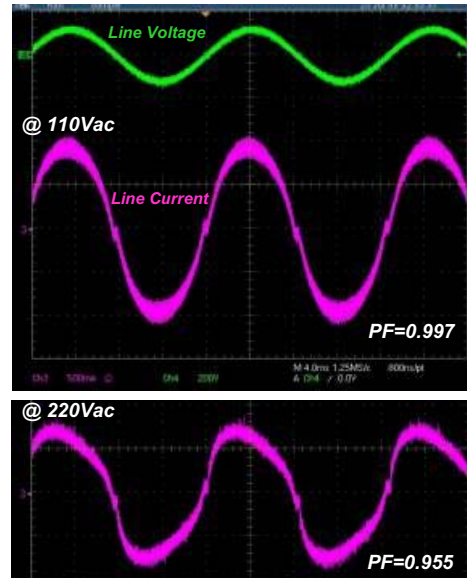**Fig. 8.** Experimental waveforms of V_{GS}, V_{DS} and I_d

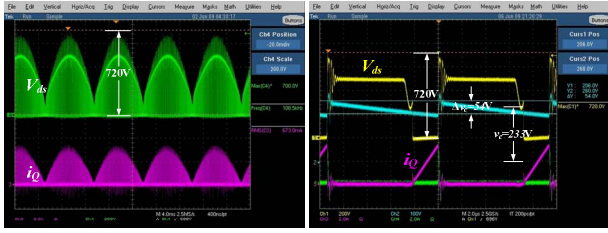**Fig. 9.** Experimental waveforms of input voltage and current

I-290

Fig. 10. Drain-source voltage and switching current at 265Vac input condition
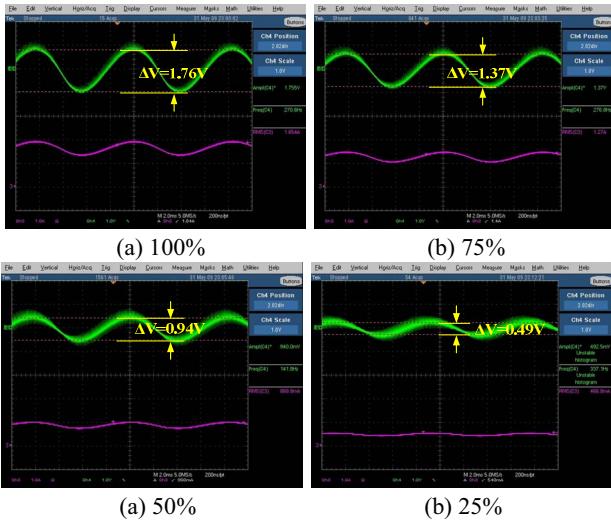

(a) 100%   (b) 75%

(a) 50%   (b) 25%

Fig. 11. Output voltage and current for load variation

The photograph of experimental set-up is shown in Figure 7. The electrical parameters are listed in Table 1. Figure 8 shows the experimental waveforms of V_{GS}, V_{DS} and I_d at $110V_{ac}$ input and at 220 V_{ac} input respectively, which shows the switching current waveforms follow the sharp of the input voltage well. Figure 9 shows the input voltage and current at 110 V_{ac} input and 220 V_{ac} input conditions. The power factors at 110 V_{ac} and 220 V_{ac} condition are measured as 0.997 and 0.955 respectively. To suppress the surge voltage of MOSFET caused by the resonant between L_{leak} and C_{oss}, RCD snubber circuit is necessary. The snubber voltage is estimated as 1.5 times of the flyback voltage and the ripple voltage is estimates as 50V. The snubber resistor and capacitor are determined by following equations;
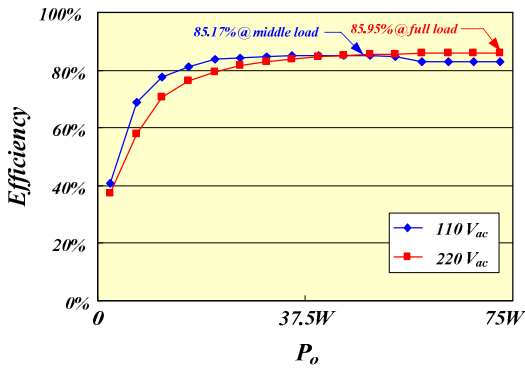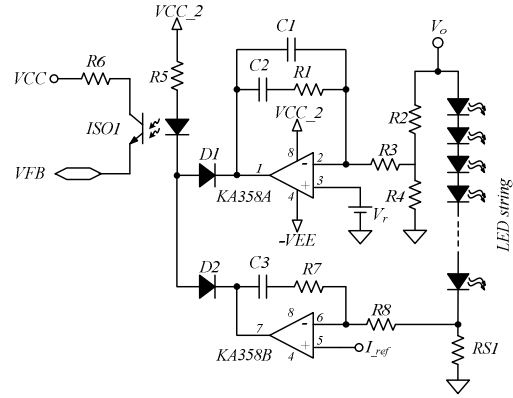

Fig. 12. Efficiency comparison

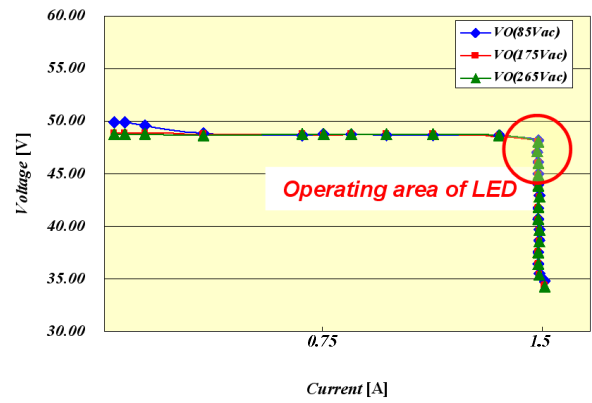**Fig. 13.** Constant current and constant voltage feedback circuit

Fig. 14. Output *V-I* characteristic

$$I_{Dsn\_pk@V_{in}=265V} = \frac{2\sqrt{2}P_o}{\eta D_{min}V_{in}} = \frac{2\sqrt{2}\times75}{0.85\times0.33\times265} = 2.85A \quad (14)$$

$$V_{sn(max)} = 1.5V_f = 1.5\times\frac{N_1}{N_2}V_{o\_Limit}$$
$$= 1.5\times\frac{44}{17}\times50 = 194.1V \quad (15)$$

$$t_s = \frac{15\times10^{-6}\times2.85}{194.1} = 220.3n\sec \quad (16)$$

$$f_{s@v_{in}=265V} = \frac{D_{min}V_{sn(max)}}{L_m I_{Dsn\_pk@V_{in}=265V}}$$
$$= \frac{0.33\times194}{297\times10^{-6}\times2.85} = 75.63kHz \quad (17)$$

$$R_{sn} = \frac{2\times194^2}{15\times10^{-6}\times2.85\times75.63kHz} = 23.3k\Omega \quad (18)$$

$$C_{sn} = \frac{V_f + V_{sn}}{\Delta v_c \times R_{sn} \times f_{s@v_{in max}}}$$
$$= \frac{194+129}{50\times23.3\times10^3\times75.63\times10^3} = 3.67nF \quad (19)$$

From the result, $3 \times 2W$ $71k\Omega$ resistors, 4.7nF/1kV capacitor and UF4005(UFRD) are finally chosen for the snubber circuit. Figure 10 shows the waveforms of the drain-source voltage and

current when the AC input voltage is 265V, the maximum voltage. The voltage ripple is measured as 54V and the maximum voltage stress is 720V, which shows the actual results are approximately in accord with the calculation. However, the maximum voltage is 720V, 800V rating MOSFET is consequently needed for wide input voltage range. Figure 11 shows the waveforms of the output voltage and current for load variation. The output voltage ripple at 100%, 75%, 50% and 25% load condition is 1.76V, 1.37V, 0.94V and 0.49V respectively. The maximum ripple at 100% load condition is 3.67% of the normal output DC voltage and the 120Hz current ripple is observed. However, since the output current is continuous and the ripple frequency, 120Hz is sufficiently high, the flicker phenomenon is invisible to human eyes. The efficiency characteristics according to the load variation for the input voltages, 110 V_{ac}, and 220 V_{ac} conditions are plotted in Figure 12. The maximum efficiency is measured as 85.17% at the middle load condition in the case of 110Vac input and 85.95% at full-load condition in case of 220Vac input respectively. Figure 13 shows a CV and CC mode feedback circuit applied to the prototype single stage flyback converter experimental set-up for LED lighting. Since the forward voltage drop of LED decreases as the junction temperature increases, LED strings have to be driven by the constant current mode. Figure 14 shows the *V-I* characteristics of the prototype experimental set-up. From the result, it is clearly verified that the output is driven well by the constant current control for whole input voltage condition.

4. Conclusion

In this paper, a single stage flyback converter for the high power LED lighting applications is presented and its operation principal was analyzed. Even though the circuit has simple structure, it can achieve high power factor, over 0.95, for whole input voltage condition. To verify the validity of the single stage flyback converter for LED lighting, an experimental set-up was built. As a result, the maximum power factor is 99.7% and the maximum efficiency is 85.95% respectively.

5. References

[1] H. van der Broeck, G. Sauerländer and M. Wendt, "Power driver topologies and control schemes for LEDs", IEEE APEC 2007, pp. 1319-1325.

[2] Zhongming Ye; Greenfeld, F.; Zhixiang Liang, Design considerations of a high power factor SEPIC converter for high brightness white LED lighting applications, Power Electronics Specialists Conference, 2008, June 2008, pp2657 - 2663 J.

[3] Xiaohui Qu; Wong, S.C.; Tse, C.K.; Xinbo Ruan, Isolated PFC Pre-Regulator for LED Lamps, Industrial Electronics, 2008. IECON 2008, Nov. 2008 pp 1980 – 1987

[4] Zhongming Ye; Greenfeld, F.; Zhixiang Liang, A topology study of single-phase offline AC/DC converters for high brightness white LED lighting with power factor pre-regulation and brightness dimmable, IECON 2008, Nov. 2008, pp 1961 – 1967

[5] H. Wei and I. Batarseh, "Comparison of basic converter topologies for power factor correction," in Proc. Southeastcon'98, 1998, pp. 348-353.

[6] Yongqiang Zheng; Moschopoulos, G., Design considerations for a new ac-dc single stage flyback converter, APEC '2006, March 2006

[7] Shen Miaosen; Kang Wanying; Qian Zhaoming, A novel average model for a single stage PFC converter, Computers in Power Electronics, 2000, July 2000 pp 151 - 156

[8] Datasheet; FAN7530 Critical conduction mode PFC controller [Fairchild semiconductor], Available; http://www.fairchildsemi.com/pf/FA/FAN7530.html